Acta Geochim (2018) 37(3):402–413
https://doi.org/10.1007/s11631-017-0258-z

ORIGINAL ARTICLE

Using electrogeochemical approach to explore buried gold deposits in an alpine meadow-covered area

Panfeng Liu[1,2] · Xianrong Luo[1,2] · Meilan Wen[1,2] · Jiali Zhang[1] · Wen Gao[1,2] · Fei Ouyang[1,2] · Xuchuan Duan[1]

Received: 9 September 2017 / Revised: 26 October 2017 / Accepted: 26 December 2017 / Published online: 23 February 2018

Abstract Exploration for buried gold ores and other deeply buried ores, especially in high altitude localities, is one of the tough challenges facing the geological world today. Fast and efficient ore prospecting methods are badly needed to deal with the situation. This paper documents a test that, for the first time, uses an electrogeochemical approach to prospect ores in the alpine meadow-covered Bangzhuoma area and its periphery in Qinghai–Tibet Plateau. The results were compared with conventional soil measurements from a 2D prospection, and an ideal model of electrogeochemical anomaly formation in the area was established based on the comparison in order to provide theoretical guidance to buried ore prospecting in areas with similar conditions. The research shows that: (1) For exploration of deeply-buried mineral deposits, an electrogeochemical approach is better than soil measurements in terms of correspondence between element content values and anomaly forms and spatial distribution of known deposits in sections. Anomalies of high to low temperature element associations (Bi–Mo; Au–Ag–As–Bi and Au–Ag) and clear zonation were also observed along vertical vein runs in the sections. Based on integration of the observation with geological characteristics of the sections, we propose to use Au, Ag and As as the electrogeochemical indicators and Bi and Mo as the electrogeochemical tracing elements to guide further analysis. (2) Judging from element statistics and the scale, intensity, and range of anomalies in plan maps, we found that an electrogeochemical approach is less affected by topography and secondary actions. The plan maps also show that elemental differentiation coefficients of the study area are in an ascending order of Ag (0.67) < Mo (0.85) < Bi (0.97) < Au (1.51) < As (2.35), better representing the element distribution in the area and yielding more striking and concentrated anomalies for known deposits than that of the soil measurements. Apart from that, electrogeochemical anomalies were observed in the south of lines 002 and 003 and the central of lines 008 and 009. We suggest the existence of deeply-buried mineral deposits based on analyses of element combinations and gold grade variations in samples taken from exploratory trenches in the area. (3) A three-stage (referring to the ore body dissolution, the mineralogenetic particle migration, and the mineralogenetic particle unloading) electrogeochemical ideal model was established for the study area, which takes into account moderate rainfall, high altitude, low air pressure, well-developed vegetation and roots, and an Upper Triassic Nieru Formation carbonaceous sandy slate as overburden.

Keywords Electrogeochemistry · Buried mineral deposit · Ideal anomaly model · Alpine-meadow covered · Ihunze

✉ Xianrong Luo
lxr811@glut.edu.cn

Panfeng Liu
1056763179@qq.com

[1] Earth Sciences of Guilin University of Technology, Guilin 541006, China

[2] Research Institute of Prediction of Hidden Deposits, Guilin University of Technology, Guilin 541006, China

1 Introduction

Electrogeochemical prospection, one of the deep-penetration geochemical exploration approaches, effectively works in pinpointing concealed deposits or ones that are hard to locate with other prospecting methods. It is based on a theory proposed by Safronov N.I., a Soviet researcher,

who suggested that an artificial electric field could act on orebodies deeply buried in the Earth and force metal ions contained within these orebodies to transport them to surface. The theory, together with its technology application on mineral exploration, was documented and published first in 1973 (Ryss and Goldberg 1973). In 1978, Soviet began to use the method in exploration for Cu–Ni, W–Mo, and gold ores buried at a depth between 600 and 800 m, and also for oil and gas reservoirs of 2000–3000 m deep (Ryss et al. 1990). It was not until 1985 that the method had been introduced to other countries, including India, Canada, the U.S., and Australia (Shmakin 1985; Salapatra et al. 1986; Govett and Atherden 1987; Ryss and Siegel 1992; Smith et al. 1991, 1993). Later, U.S. expert Leinz R.W. and Israeli scholar A. Levitski made improvements to the extraction device of the method and proposed the so-called "NEO–CHIM" and "Dipole CHIM" approaches, respectively, to better apply these method to ore deposit survey (Leinz and Hoover 1994, Leinz et al. 1998; Levitski et al. 1996).

In the late 1970s, several Chinese researchers, including Fei Xiquan and Xu Bangliang, blazed a trail in electrogeochemical exploration in China by introducing the concept into the country and publishing papers on the issue in Chinese journals including *Geophysical and Geochemical Exploration* and *Geology and Prospecting* (Fei 1984; Xu et al. 1984). Since then, and especially after 2000, electrogeochemical exploration has been applied and advanced in China, gradually forming a technology featuring low-voltage, dipole, and independent power supply. The technology can be used to find ore deposits or perform assessment of the deposits through metal ion anomalies related to ore deposits. It relies upon an external electric field to move metal ions that were already transported to the Earth's surface to assigned extraction electrodes, and then collects and analyzes the electrolytes on the adsorbing materials of the electrodes (Luo et al. 2002a, b; Kang and Luo 2003). The technology was applied to various regions covered by dry deserts, forests, prairies, and swamps, with positive results achieved (Chen et al. 2007; Shu et al. 2009; Wang et al. 2011; Yan et al. 2014). This paper documents an electrogeochemical exploration test in the Bangzhuoma gold deposit covered by alpine meadow in Tibet Plateau and compares the results (sections and planes) with that of conventional soil measurements to further demonstrate the reliability and efficiency of the technology.

The study area is located in a high mountain region with an average elevation of 4800 m, in Longzi County, Shannan Prefecture of Tibet Automonous Region, China. It is higher in the north and west and lower in the south and east. Featuring low temperature, wide-spreading tundra, an annual precipitation of 297.41 mm and less evaporation, the area is mostly covered by 10–20 cm-thick sods of well-developed roots (Fig. 1).

The area sits on the Himalayan block at the southern part of the Tibet Plateau and the central-eastern part of the Himalayan Tethys orogenic belt. It is defined to the north by the Yarlung Zangbo River structure zone (Fig. 2a) (Zheng et al. 2004; Wang et al. 2013). The area contains complicated structures as a result of intensive magmation and metamorphism as a result of the Himalayan orogeny. It is a second order tectonic unit of the Kangma-Longzi fold belt and sandwiched by an extension-detachment fault and the Gudui-Longzi fault. The Yelaxiangbo metamorphic core complex developed in the north of the area is the Miocene binary mica and monzonitic granite. The Zhegu-Ridang fold thrust bundle in the south of the area contains Late Cretaceous diabase dyke swams, which provide partial heat source for metallogenic thermal fluids rising along faults, folds or other tectonic structures (Wang et al. 2013). The intensive collision orogenesis between the Himalayan Block and the Gangdise Block and the subsequent large-scale extension and detachment are regarded as important factors behind the formation of the Zhegu Au–Sn deposit in the western part of the area and the Mazala gold ore and Zhaxikang lead zinc ore in the southern part of the area, now an important Au–Sn metallogenic belt in the Tibet Plateau (Fig. 2b) (Du et al. 1993; Nie et al. 2005, 2006).

There is only one strata-the Nieru Formation of the Triassic (T_3n)—outcropped in the study area. In the northwestern and central southern parts, the second member of the Formation(T_3n^2) contains dark grey to black layers of sericite silty slates with some laminas of greywacke; in the central part, the third member of the Formation(T_3n^3) has wide-spreading grey-dark grey silty sericite slates interbedded with medium-thick fine-grained metamorphic feldspar and quartz greywacke; and the fourth member of the Formation (T_3n^4) also exposes a little as grey silty sericite slates interbedded with thick-massive layers of metamorphic feldspar and quartz greywacke. Faults in the area mostly extend in nearly east-westward and north-westward directions. The former is represented by the Sederenjin-Duolazeri fault (F2)—a low angle thrust nappe structure—and a series of secondary faults (F4, F6), which are the main ore-controlling structures and spatial location to most mineralization alteration zones in the area. The latter is represented by the Xinna fault, a trust fault (F5) (Dong et al. 2012; Chen et al. 2016). Nine gold veins and five gold ore bodies were delineated in the Bangzhuoma mining area. The major veins are ③, ④ and ⑤ veins with strike length ranging between 900 and 1300 m and Au grade between 1.02×10^{-6} and 5.47×10^{-6}. They occur mainly in fractured alteration zones with altered sandstone/quartz veins. The mineralization types include arsenopyritization, pyritization, and ferritization, and the alteration

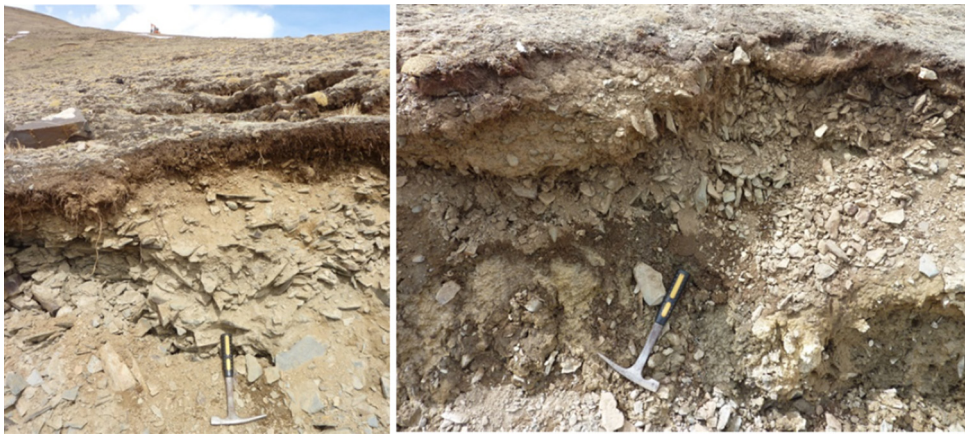

Fig. 1 Geomorphic features of areas covered by alpine meadow

types are largely silicification and carbonatization (Chen et al. 2016).

2 Method and technology

2.1 Sampling

A prospecting study was carried out in areas with available prospecting lines with a total length of 1000 m and 170° strike angle in the Bangzhuoma mining area and its periphery. Ten sampling lines labeled from 001 to 010 were laid out. Sampling was performed every 40 m inside the mining area and every 200 m × 40 m in the periphery. For sampling points with basement crops, sampling was deviated east-westward normally less than 10 m from being perpendicular to the sampling lines. Electrogeochemical samples as well as soil samples were taken at each sampling point.

For electrogeochemical extraction, we used the dipole CHIM extraction device with independent power supply developed by Buried Ore Deposit Research Institute of Guilin University of Technology (Fig. 3). The extraction process lasted for 48 h with 1000 mL of extracting solution at a voltage of 9 V. Electrodes were buried in B layer (the illuvium horizon, Fig. 3) with a depth of 30–50 cm. Extraction electrodes were placed 100 cm apart, and extraction material was treated in high-density foamed plastic. The soil sampling depth was the same as the electrodes, and samples were sieved with a 20 mesh sifter.

2.2 Analysis method

Electrogeochemical samples (extracted with foamed plastic) and soil samples were tested with a U.S.-made X-series inductively coupled plasma mass spectrometer in the Test Center of China Nonferrous Metals (Guilin) Geology and Minging Co., Ltd.

The test was carried out with the following conditions: ICP power: 1300 W, cooling air flow rate (Ar): 13.0 L/min, auxiliary air (Ar) flow rate: 0.90 L/min, atomization air (Ar) flow rate: 0.76 L/min, sampling cone size (Ni): 1.0 mm, skimming cone size (Ni): 0.7 mm,resolution: 05–0.1 aum, test mode: peak jumping,analysis mode: pulse counting, sampling depth: 60 Step, scan times: 50, dwell time: 10 ms, sample uptake rate: 1.0 m, and quality channel number: 3 (Shi et al. 2009).

3 Results

3.1 Section comparison

Table 1 lists test results of electrogeochemical and soil samples taken from layers above the exploratory lines in Bangzhuoma mining area. Figure 4 shows anomalies of each element with corresponding sections.

1. Original data comparison shows order of magnitude difference between test data of the two kinds of samples. For instance, the electrogeochemical sample measurement yielded the maximum As value of 32.91 μg/g, which was equal to the minimum value of As for soil sample measurement. The maximum As value for the soil sample was as high as 85.71 μg/g. Analyses of curve shapes and angles indicate that electrogeochemical measurements produce more single- or multiple-peak anomalies with local trapezoid shapes and can be used to reveal the locations of shallow veins and their extension directions. Meanwhile the soil sample measurements yielded mostly single peaks, revealed only the locations of shallow veins (no response to deep veins). The method also appeared to be easily affected by secondary actions.
2. Analyses of correspondence between anomalies and locations of veins showed that samples from No. 8 to

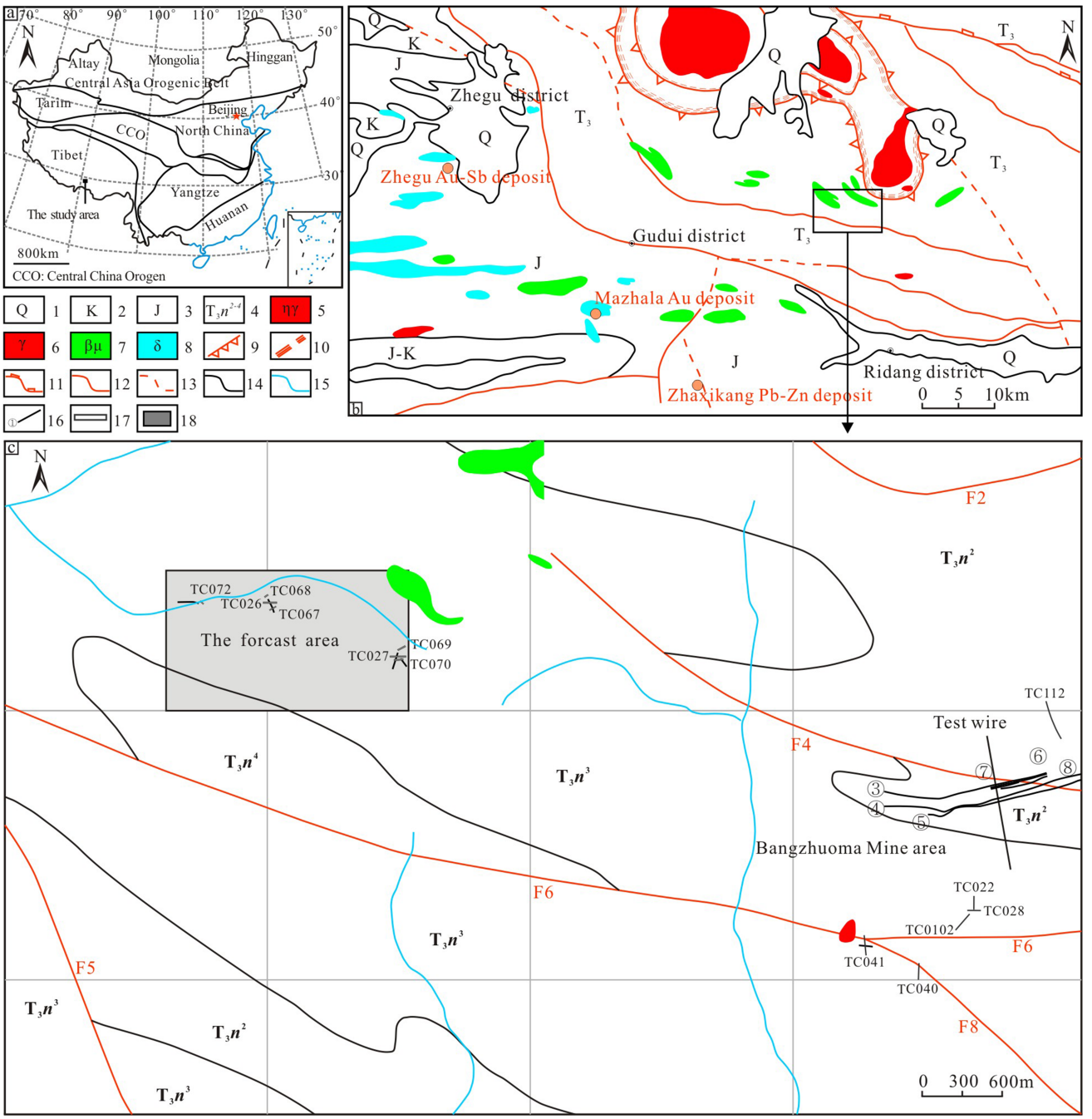

Fig. 2 Simplified maps of relevant geotectonic structures and the study area. **a** Approximate location of relevant geotectonic elements, **b** outline map of structure elements in the study area, **c** outline map of the mining area. 1. Quaternary glacier, alleviation and lacustrine deposits, 2. cretaceous marine clastic rocks, 3. Jurrasic marine clastic rocks, 4. second to fourth members of the Upper Triassic, 5. binary and monzonitic granite, 6. quartz diorite, 7. sillite, 8. diorite 9. extension-detachment fault, 10. ductile shear zone, 11. plate stylolite, 12. fault line, 13. deduced fault line, 14. geological boundary, 15. river, 16. revealed veins and their serial numbers, 17. exploratory trench, 18. location of the study area

No. 14 prospecting lines had their elements Au, Ag, As and Bi corresponding well to the locations of cropped veins, samples from No. 3 to No. 5 prospecting lines had their Au and Ag indicating the locations of veins buried in deeper layers, and samples from No. 17 to No. 19 prospecting lines had their Bi and Mo providing clues by forming three element combinations through giving signals of Au–Ag,Au–Ag–As–Bi, and Bi-Mo perpendicular to veins. Only soil samples from No. 10 to No. 14 prospecting lines were measured to have elements of Au, Ag, As, Bi and Mo, corresponding well to outcropped shallow veins, and the anomalies

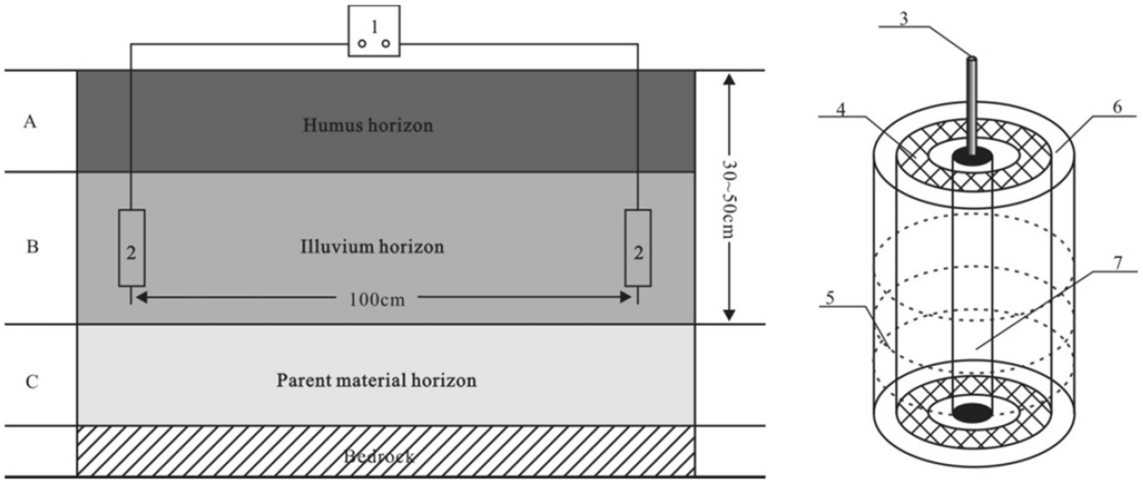

Fig. 3 Diagrams showing sampling methods and the dipole CHIM extraction device with independent power supply. 1. Controllable power source, 2. extraction electrodes, 3. connecting wire, 4. adsorptive foamed plastic material, 5. fixed wire, 6. filter paper, 7. graphite carbon rod

Table 1 Test results of electrogeochemical and soil samples above the No. 4 prospecting line in Bangzhuoma mining area

Nom	Geo-electric chemistry measurement					Nom	Soil measurement				
	Au	Ag	As	Mo	Bi		Au	Ag	As	Mo	Bi
T-1	6.67	0.020	11.95	0.155	0.068	S-1	12.63	0.113	318.36	1.48	1.26
T-2	4.58	0.029	2.31	0.053	0.066	S-2	5.45	0.137	242.75	1.36	1.21
T-3	6.51	0.030	3.86	0.055	0.042	S-3	2.97	0.126	158.53	1.23	1.10
T-4	7.46	0.045	1.87	0.039	0.035	S-4	2.32	0.105	81.83	1.35	1.03
T-5	9.97	0.032	2.26	0.048	0.037	S-5	2.95	0.126	135.29	1.39	1.21
T-6	2.54	0.030	3.45	0.039	0.043	S-6	3.57	0.146	188.74	1.43	1.38
T-7	6.78	0.026	5.13	0.064	0.057	S-7	2.91	0.143	92.71	1.15	1.01
T-8	8.27	0.045	13.01	0.102	0.101	S-8	3.44	0.141	139.38	1.09	1.02
T-9	20.25	0.050	16.95	0.174	0.177	S-9	3.04	0.115	207.95	1.13	1.27
T-10	8.84	0.017	19.81	0.119	0.074	S-10	6.24	0.098	295.61	1.09	0.96
T-11	5.61	0.052	32.91	0.17	0.143	S-11	49.22	0.481	585.71	3.10	2.74
T-12	3.26	0.022	14.66	0.123	0.12	S-12	4.27	0.131	175.63	1.33	1.05
T-13	16.22	0.038	4.65	0.068	0.036	S-13	4.63	0.132	247.05	1.57	1.56
T-14	15.67	0.029	26.25	0.142	0.172	S-14	54.77	0.140	374.21	1.90	1.78
T-15	6.71	0.029	10.16	0.101	0.083	S-15	25.54	0.149	342.76	1.51	1.75
T-16	6.15	0.034	14.87	0.084	0.096	S-16	28.47	0.169	353.83	1.29	0.99
T-17	6.71	0.036	10.91	0.153	0.122	S-17	4.51	0.083	97.48	1.33	0.70
T-18	7.34	0.028	12.71	0.294	0.195	S-18	2.19	0.083	37.99	1.27	0.66
T-19	10.34	0.023	5.22	0.115	0.1	S-19	2.19	0.102	43.63	1.40	0.92
T-20	9.68	0.029	2.07	0.049	0.036	S-20	2.13	0.104	41.50	1.27	0.92
T-21	4.31	0.034	4.59	0.129	0.072	S-21	2.84	0.096	34.14	1.39	0.81
T-22	1.96	0.019	3.93	0.098	0.063	S-22	1.69	0.087	32.73	1.45	0.80
T-23	8.31	0.019	4.02	0.127	0.073	S-23	1.94	0.113	30.92	2.34	0.80
T-24	3.37	0.014	2.79	0.058	0.031	S-24	2.58	0.092	31.04	2.99	0.73
T-25	7.09	0.023	2.46	0.059	0.046	S-25	1.94	0.101	36.69	1.28	0.85
T-26	5.15	0.013	2.36	0.06	0.043	S-26	1.87	0.084	33.91	1.31	0.80

Au: ng/g, and all the other elements: μg/g

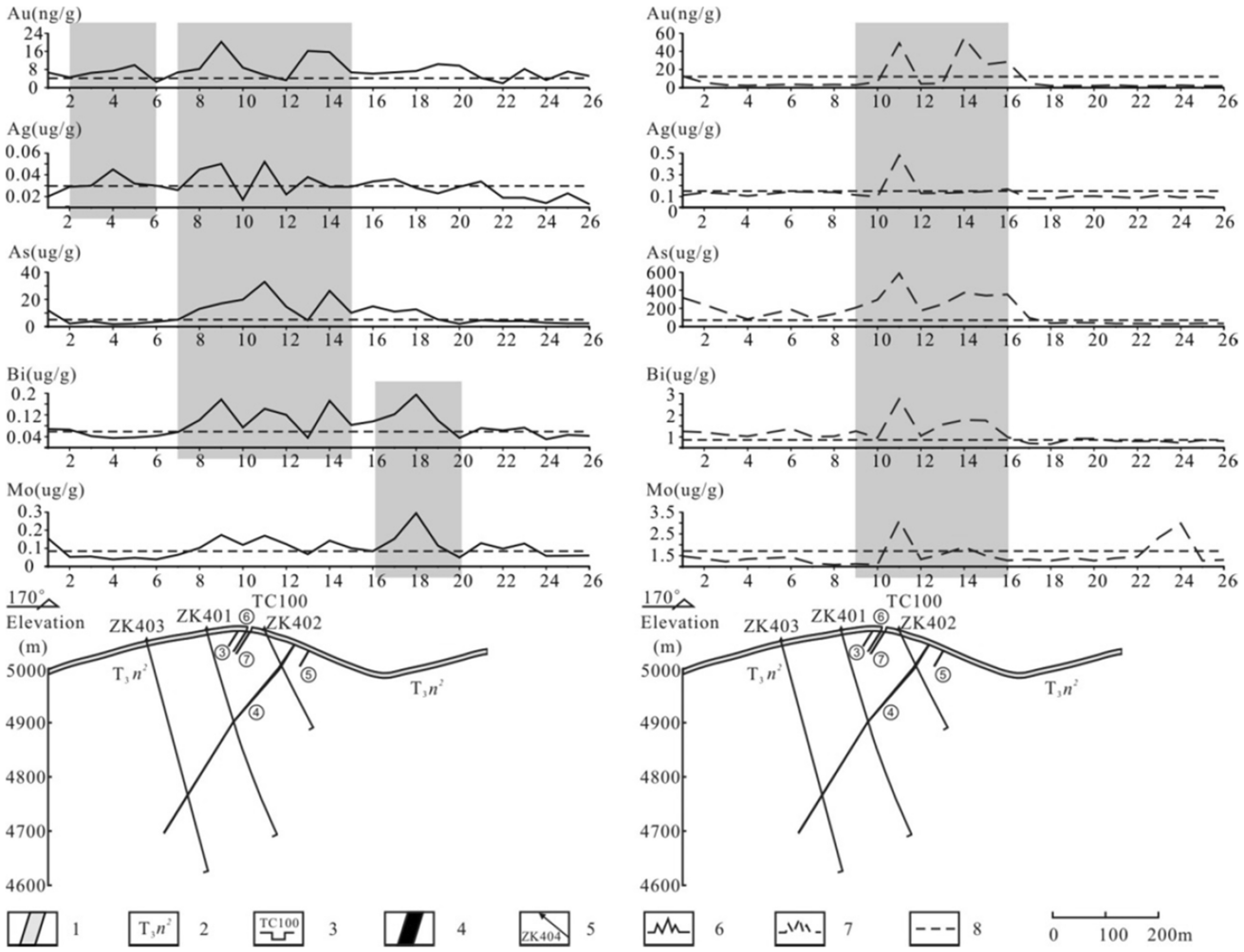

Fig. 4 Comparison of sections derived from measurements of electrogeochemical and soil samples. 1. Quaternary, 2. second member of the Nieru Formation of the Upper Triassic, 3. veins, 4. exploratory trench and serial number, 5. perforation and serial number, 6. electrogeochemical anomalies, 7. soil measurement anomalies, 8. background value line

had smaller widths than those in the electrogeochemical samples.

3.2 Plane comparison

Section comparisons can be used to assess the effectiveness of exploration and determine indicative element combinations through aspects of element content and curve shape. However, information such as element characteristics, the abnormal spatial distribution, and intensity and range of elements, is acquired through statistics of element content and abnormal element planes based on plane comparison.

3.2.1 Statistic comparison of electrogeochemical and soil measurements

Statistics of geochemical elements can be analyzed and used as indicators to ore deposits. Table 2 lists statistics of soil and electrogeochemical measurements in the periphery of Bangzhuoma mining area. It shows that:

1. Background values are important indicators of geochemical anomalies. However, element contents of the samples are sometimes extremely high or low, causing the background values for both measurements to be lower than the average element content values.
2. The difference between the maximum and minimum values was more obvious in electrogeochemical samples than in soil measurements. For example, the content of Au in electrogeochemical samples ranged between 0.03 and 105.40 μg/g, which was 3515 times apart. In contrast, the soil samples had an Au content range of 1.2 and 119 μg/g, only 99 times apart between the maximum and the minimum. The maximum and minimum content values of element Bi in electrogeochemical samples (56 times) were also many more times apart than that in soil samples (5.8 times),

Table 2 Statistics of element content in electrogeochemical and soil samples from the periphery of the Banzhuoma mining area

Element	Electrogeochemical measurement					Soil measurement				
	Au	Ag	As	Mo	Bi	Au	Ag	As	Mo	Bi
Maximum	105.40	0.165	371.00	0.852	0.668	119	1.670	3505	5.76	2.48
Minimum	0.03	0.003	1.07	0.019	0.012	1.2	0.049	27	0.75	0.43
Average	5.95	0.036	11.44	0.117	0.084	21.14	0.192	180.03	2.05	0.83
Standard deviation	8.99	0.024	26.92	0.099	0.081	21.86	0.167	337.29	0.86	0.28
Variation coefficient	1.51	0.67	2.35	0.85	0.97	1.03	0.87	1.87	0.42	0.33
Background value	3.92	0.032	4.78	0.093	0.064	12.94	0.15	60.95	1.90	0.75

Au: ng/g and all the other elements: μg/g

indicating a higher dispersion degree in the former samples than the latter, thus better representing the distribution of elements in the area.

3. The average element content values of electrogeochemical samples were orders of magnitude lower than that of soil measurements, which was consistent with the results of section analyses of the two kinds of samples. To reduce the effect of measurement scale and dimension upon the differentiation of elements in the area, we calculated the differentiation coefficients (standard deviation/average value) of each element and listed them in Table 2. From Table 2 and Fig. 5, we have differentiation coefficients of elements for electrogeochemical and soil samples in an ascending orders of Ag (0.67) < Mo (0.85) < Bi (0.97) < Au (1.51) < As (2.35) and Bi (0.33) < Mo (0.42) < Ag (0.87) < Au (1.03) < As (1.87), respectively. The differentiation coefficients of Au and As for both kinds of samples were bigger than 1, which meant high differentiation and possible mineralization of gold in certain parts of the area. The differentiation coefficients of Ag, Mo and Bi in electrogeochemical samples ranged between 0.5 and 1, meaning medium differentiation. Meanwhile those in soil samples were all less than 0.5, indicating low differentiation or no differentiation at all. This shows that electrogeochemical samples yield more differentiated element results.

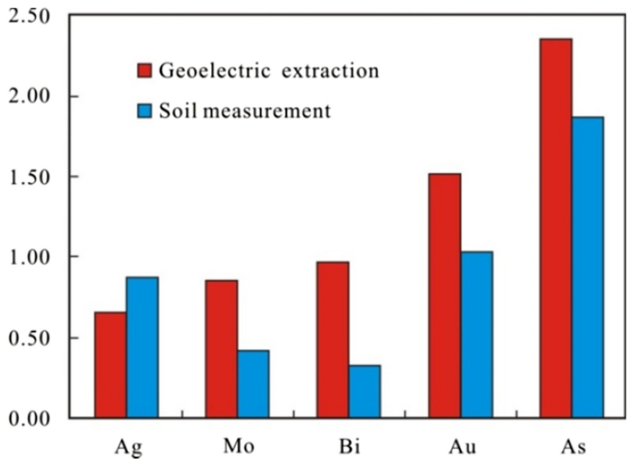

Fig. 5 Comparison of element differentiation coefficients of electrochemical and soil samples from the periphery of Bangzhouma mining area

3.2.2 *Comparison of plane anomalies in electrogeochemical and soil measurements*

To better compare the plane anomalies of electrogeochemical and soil measurements, we used "single-point anomaly contrast value" of 1.2 and 2.5 as contour line to map the anomalies with the universal Kring method.

The single-point contrast value (K, dimensionless) refers to the ratio of the original value to the background value of certain elements in each sampling point. With K larger than 1, we may presume relative enrichment of elements, and with K less than 1, we may infer relative depletion of elements (Zhang et al. 2015; Li et al. 2016). The value is therefore used to indicate the enrichment or depletion of certain elements. It may be represented by an equation of $K = C/C0$, in which K is the single-point contrast value, C is the content of certain element, and C_0 is the background value of certain element.

Anomaly contrast shows how clear an anomaly is. It can be used not only as an anomaly marker but also to eliminate interference caused by background value differences and to compare anomaly scale and enrichment degree of different elements in samples. Figures 6 and 7 are plane graphs of anomaly contrast of elements Au, Ag, As, Mo and Bi, derived from soil and electrogeochemical measurements. It can be concluded from the figures that:

1. It is topographically higher in the south than the north and the east than the west within the study area. A deep V-shaped gully with running water of near E–W direction winds in the north and two V-shaped gullies of near S–N direction run in the south. Soil measurement anomalies are mostly from the lower northwest part (probably affected by the topography). The

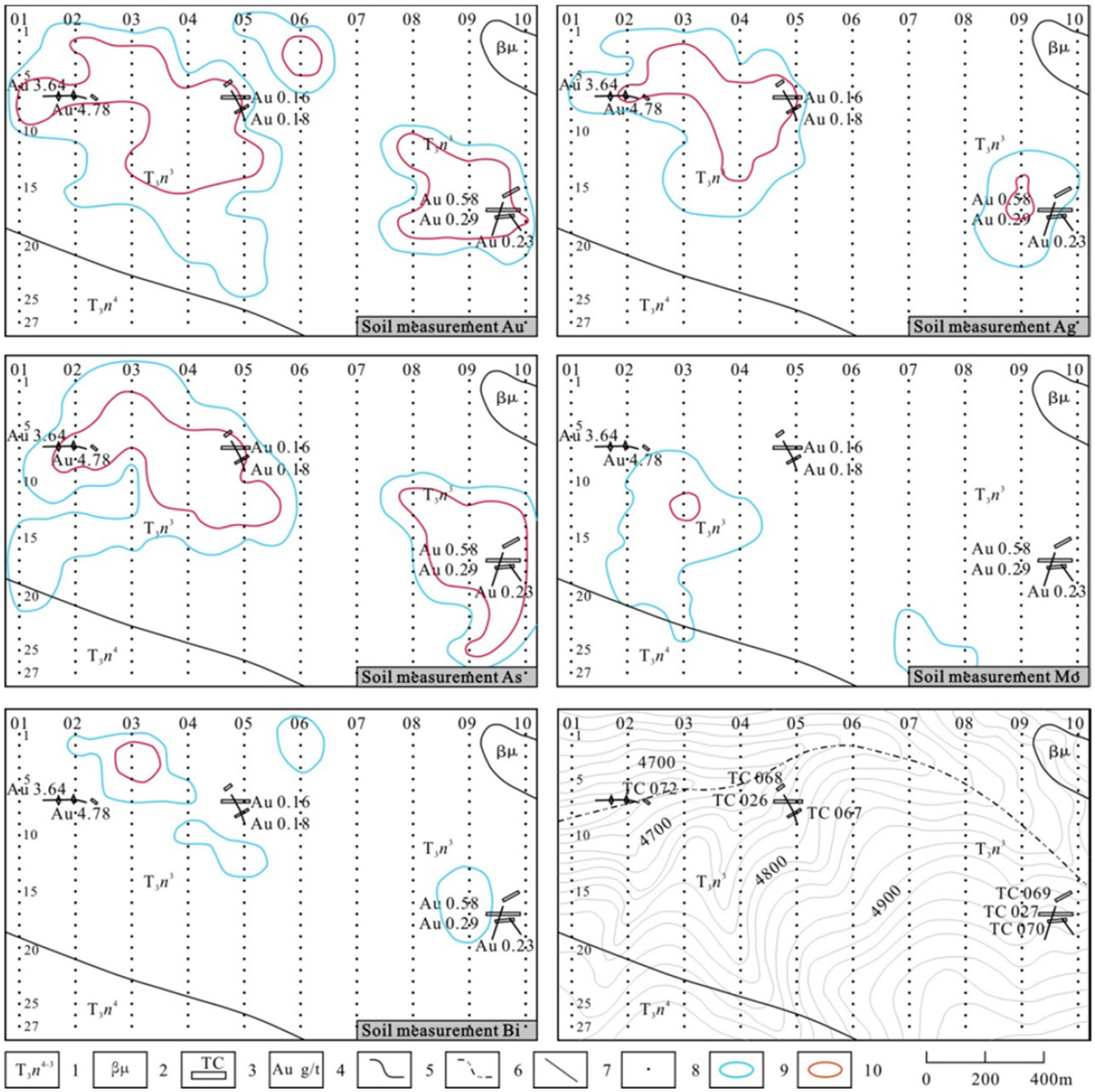

Fig. 6 Plane maps of contrast anomalies of elements from soil measurements. 1. Third to fourth members of the Upper Triassic Nieru Formation, 2. diabase vein, 3. exploratory trench, 4. gold grade, 5. geological boundary, 6. river, 7. vein, 8. sampling point, 9. 1.5 isoline of contrast anomalies, 10. 2.5 isoline of contrast anomalies

anomalies of elements Au, Ag and As occupy larger areas and are higher in values. However, the correspondence between these anomalies and revealed veins are not as strong due to secondary actions and topography. Elements Mo and Bi generate small-area anomalies and low values and thus are worthless as indicators.

2. Anomalies of elements derived from electrogeochemical sample measurements have several high-value areas, showing no clear sign of being affected by topography. Elements Au and Ag not only generate anomalies matching well with revealed veins but also show significant anomalies along lines 003 and 004 and in parts of lines 008 and 009. Element As yields

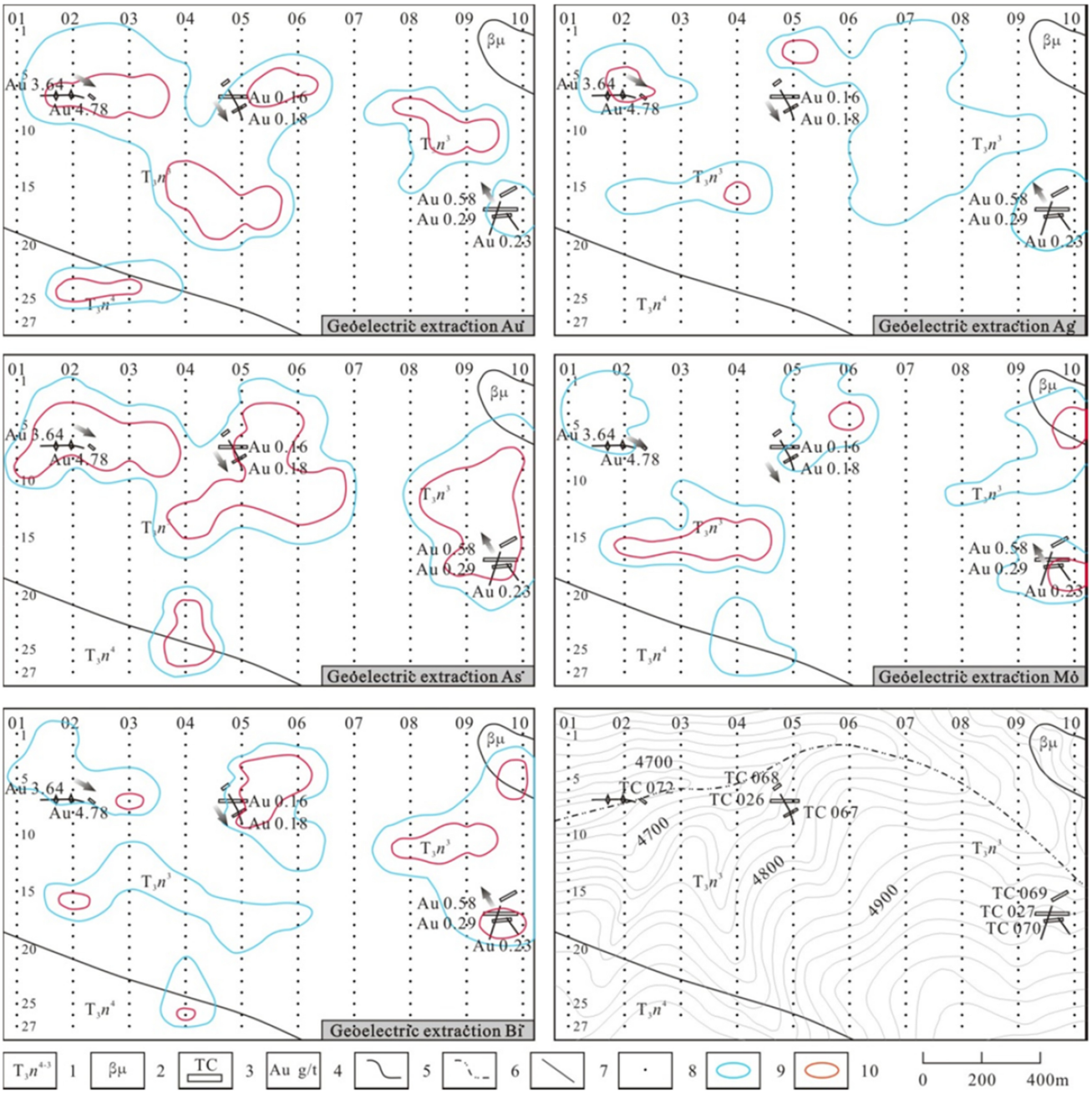

Fig. 7 Plane maps of electrogeochemical contrast anomalies of elements in the study area. 1. Third to fourth members of the Upper Triassic Nieru Formation, 2. diabase vein, 3. exploratory trench, 4. gold grade, 5. geological boundary, 6. river, 7. vein, 8. sampling point, 9. 1.5 isoline of contrast anomalies, 10. 2.5 isoline of contrast anomalies

large-area anomalies and higher anomaly values, with anomalies along line 004 corresponding well with revealed veins and synchronized with (weaker) anomalies of elements Mo and Bi at the third and fourth members of the Nieru Formation at the south part of the line 004. Elements Ag, Mo, and Bi yield anomalies simultaneously at measure points 14–17 of lines 002, 003 and 004; elements Au, As, and Bi yield anomalies at measure points 10–15 of lines 008 and 009.

3. The Au grade changes obviously in measure points and in ongoing exploratory trenches of known gold mineralization and revealed veins (Fig. 7) in the study area. The grade rises from 3.64 to 4.78 g/t from measure points D1 to D2 and is 0.29 and 0.23 g/t for two veins within TC070, respectively. Enrichment of Au is more obvious in TC027, where the Au grade is 0.58 g/t.

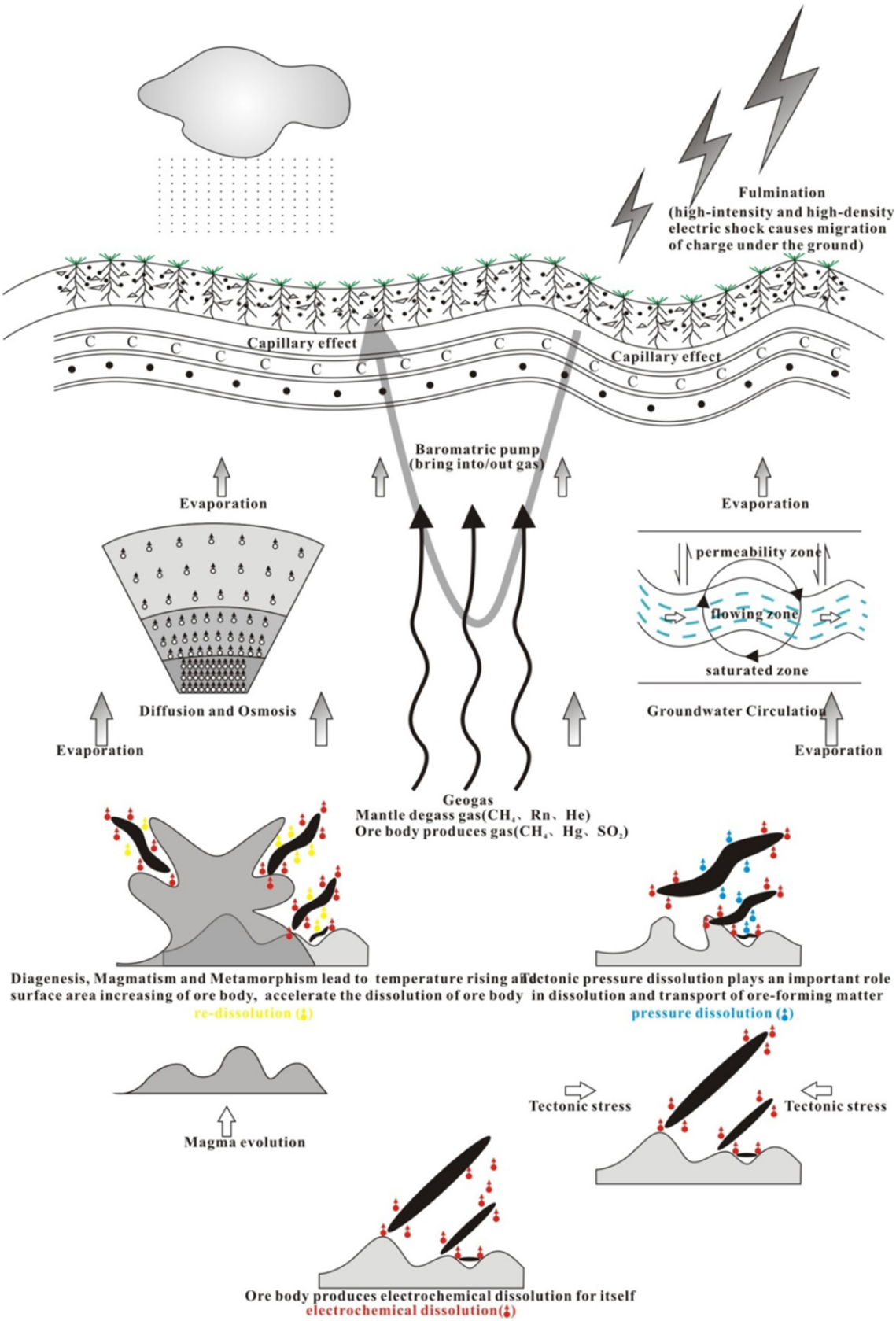

Fig. 8 Ideal model of electrogeochemical anomaly formation in alpine meadow-covered areas

4 Discussions

Element anomalies derived from soil measurements are mostly single peaks and easily affected by secondary actions. They are only good at defining the locations of shallow veins, shows no obvious anomalies to deeper ones. Au anomalies are the most common ones in the plane, corresponding well to revealed veins. Ag and As anomalies are similar. Mo and Bi anomalies are rare and are only present in outcropped veins, indicating a limitation of applying soil measurements in the area.

In contrast, electrogeochemical measurements generate high- to low-temperature anomaly associations of Bi-Mo, Au–Ag–As–Bi, and Au–Ag with vertical veins with obvious zonation. Combining the facts that gold mineralization and arsenopyrite mineralization occur in the second member of the Nieru Formation in the Upper Triassic (T_3n^2), we suggest that the Formation contains a set of semi-pelagic slope flysch association of dark black–black laminated silt-slate with high content of Au associated with unevenly distributed high-grade Ag (4.25×10^{-6}). We therefore decided to use Au and Ag as major electrogeochemical indicators and As, Bi, and Mo as minor electrogeochemical indicators for defining the locations of veins in the area. In electrogeochemical plane maps, contrast anomalies of elements Au, Ag, Mo, and Bi all show corresponding anomalies to known vein, indicating reliability of the method and better results than that of soil measurements. The Au contrast anomaly with high contrast value is found at the south of lines 002 and 003. Together with synchronized anomalies of elements As, Mo, and Bi in central parts of adjacent lines 004 and 005, they form element combination anomalies. Integrating actual mineralization at the measurement points and gold enrichment at TC026 and TC067, we suggest tendency of downward extension of the vein and the possibility of deeper buried ore bodies. While synchronized anomalies of elements Au, Ag, As, Mo, and Bi in central parts of lines 008 and 009 and Au grade rising from 0.23 g/t at Tc070 to 0.58 g/t at TC027 suggest mineralization in shallow layers in the study area.

The above discussion verifies the applicability of electrogeochemical method in the study area for its effective formation and extraction of anomalies. The electrogeochemical anomalies are generated mainly through dissolution of mineralization bodies, including (1) electrochemical dissolution caused by primary battery as a result of potential difference between different minerals, (2) re-dissolution caused by temperature build-up or surface area enlargement during magmatic evolution, and (3) tectonic pre-solution. Among them, electrochemical dissolution is the most common process, during which an ionic halo is produced around mineralization bodies and then transported upwardly and continuously through diffusion, permeation, evaporation, and soil capillarity, to near surface, where it there unloads the metal ions it has carried all the way up when encountered by some geochemical barriers (such as all kinds of secondary soluble salts, clay, oxides, organic matter, and colloidal substance). The electrogeochemcial method utilizes the external electric field to transport active metal ions to assigned extraction electrodes. By collecting and analyzing electrolytes on adsorbing materials of the electrodes one can discover ion anomalies connecting with information of ore deposits. The study area is a very suitable candidate for applying this method, for it has moderate rainfall, high altitude, low air pressure, and a well-developed vegetation root system, all of which are favorable for ion halo migration. The overlying lamina of carbonaceous sandy slate in the area also provides a closed environment for the formation of electrogeochemical anomalies. It is therefore suggested that the establishment of an ideal electrogeochemical anomaly mode for the study area is a necessary theoretical preparation for exploring buried gold deposit in similar areas covered by alpine meadow (Fig. 8).

5 Conclusions

1. The electrogeochemical method works more effectively in ore deposit exploration than soil measurement in the study area. It generates data that are more representative, especially in places with complicated topography and no obvious tectonic regions.
2. By combining the fact that electrogeochemical anomalies yield low- to high temperature element combinations of Bi–Mo, Au–Ag–As–Bi, and Au–Ag along vertical veins with geological features of ore deposits in the study area, we use elements Au, Ag, and As as electrogeochemical indicators, and elements Bi and Mo as auxiliary indicators of ore deposits. Apart from revealed veins corresponding well to electrogeochemical anomalies, we also observed anomalies at the southern part of lines 004 and 005 and the central part of lines 008 and 009. Based on the observation of Au grade changing from lean to rich, we suggest the possibility of buried ore deposits in the study area.
3. A three-stage electrogeochemical ideal model was established to guide buried ore deposit exploration in regions similar to this alpine-meadow-covered area, which features moderate rainfall, high altitude, low air pressure, well-developed vegetation and roots as well as an Upper Triassic Nieru Formation carbonaceous sandy slate as overburden. The three stages refer to ore

body dissolution, mineralogenetic particle migration, and mineralogenetic particle unloading.

Acknowledgements This study was supported by the National Key Research and Development Program of China (Grant No. 2016YFC0600603).

References

Chen XQ, Luo XR, Wang XH et al (2007) Deep penetration geochemistry survey for the gold mine prospecting in Hulalin, inner Mongolia. J Guilin Univ Technol 27(04):480–483 **(in Chinese with English abstract)**

Chen DT, Chen W, Hu KW et al (2016) Geological characteristics and geochemical anomaly of Bangzhuoma gold deposit in Longzi County, Tibet. Gold 37(08):25–28 **(in Chinese with English abstract)**

Dong FQ, San J, Wang F et al (2012) Geological characteristics and genesis of gold antimony in Longzi-Gudui area, Tibet. J Sichuan Geol 32(S1):24–27 + 32 **(in Chinese with English abstract)**

Du JS, Feng XL, Chen FZ et al (1993) The Geology of She gold deposits in Xizang (Tibet). Southwest Jiaotong University Press, Chengdu, pp 150–177 **(in Chinese with English abstract)**

Fei XQ (1984) The result of experiment with method of partial metal extraction in several mining areas. Geophys Geochem Explor 8(3):162–166 **(in Chinese with English abstract)**

Govett GJS, Atherden PR (1987) Electrogeochemical patterns in surface soils-detection of blind mineralization beneath exotic cover, Thalanga, Queensland, Australia. J Geochem Explore 28:201–218

Kang M, Luo XR (2003) Improvement and applied results of geo-electrical chemistry methods. Geol Explor 39(05):63–66 **(in Chinese with English abstract)**

Leinz RW, Hoover DB (1994) Ideal CHIM with newly-developed Neo-CHIM electrode. Explore 83:10–15

Leinz RW, Hoover DB, Fey DL, Smith DB, Patterson T (1998) Electrogeochemical sampling with NEO-CHIM results of tests over buried gold deposits. J Geochem Explore 61:57–86

Levitski A, Filanovski B, Bourenko S, Sannenbaum E, BarAm G (1996) 'Dipole' CHIM: concept and application. J Geochem Explore 51:101–114

Li H, Xu GZ, Liu HZ et al (2016) Draw geochemical exploration anomaly map by the contrast method. Mod Min 06:158–159 + 162 **(in Chinese with English abstract)**

Luo XR, Chen SM, Du JB, Hu YH (2002a) Study of geo-electrochemical method in search for different hidden deposits. J Mineral Petrol 22(04):42–46 **(in Chinese with English abstract)**

Luo XR, Wang GQ, Du JB, Hu YH (2002b) The Geo-electrochemical anomaly feature mechanism and finded ore extrapolate for stibium deposit. Geol Explor 38(02):59–62 **(in Chinese with English abstract)**

Nie FJ, Hu P, Jiang SH et al (2005) Type and temporal–spatial distribution of gold and antimony deposits (prospects) in Southern Tibet, China. Acta Geol Sin 79(03):373–385

Nie FJ, Hu P, Jiang SH et al (2006) ^{40}Ar–^{39}Ar isotope age dating on biotite samples of two monzogranite occurring in the Qiongduojiang area, southern Tibet and their geological significances. Acta Petrol Sin 22(11):2704–2710

Ryss YS, Goldberg IS (1973) The method of partial extraction of metals (CHIM) for exploration of ore deposits. Methods Tech Explore 5-19

Ryss YS, Siegel HO (1992) Some results of applying Russian geo-electrochemical methods in Canada. Scintrex Ltd., Concord

Ryss YS, Goldberg IS, Vasilyeva VI et al (1990) A feasibility of geo-electrochemical technique application in exploration for oil and gas. Sov Geol 6:28–33 **(in Russian)**

Salapatra AK, Salukdar RC, De PK (1986) Electrogeochemical technique for exploration of base metal sulfides. J Geochem Explore 25:389–396

Shi YH, Yang ZP, Huang JH et al (2009) Determination of trace elements in electrical absorption prospecting polyform sample by inductively coupled plasma mass spectrometry. Spectrosc Spectral Anal 29(06):25–28 **(in Chinese with English abstract)**

Shmakin BM (1985) The method of partial extraction of metals in a constant current electrical field for geochemical exploration. J Geochem Explore 23:27–33

Shu LX, Luo XR, Wu MS et al (2009) Geo-electrochemical method for polymetal ore deposit prospecting in arid desert area—taking Yindonggou exploration of Baiyin as an example. J Guilin Univ Technol 29(04):439–444 **(in Chinese with English abstract)**

Smith DB, Hoover DB, Sanzolone RF (1991) Development and testing of the CHIM electrogeochemical exploration method. In: USGS research on mineral resources, program and abstracts. U.S. Geological Survey Circular, 1062, pp 74–75

Smith DB, Hoover DB, Sanzolone RF (1993) Preliminary studies of the CHIM electro geochemical method at the Kokomo Mine, Russel Gulch, Colorado. J Geochem Explore 46:257–278

Wang BH, Wen ML, Ou Yang F et al (2011) Features of geo-electrochemical anomaly and Pb–Zn–Ag exploration forecast in Plains—Taking Hardattolgoi Lead–Zinc–Silver polymetallic deposit of inner Mongolia as an example. J Guilin Univ Technol 31(02):192–197 **(in Chinese with English abstract)**

Wang LQ, Pan GS, Ding J et al (2013) Regional geology of Xizang autonomous region. Geological Publishing House, Beijing

Xu BL, Fei XQ, Wang HP (1984) A new kind of gold ore prospecting method—electrochemical gold sampling test. Geol Explor 10:55–59 **(in Chinese with English abstract)**

Yan W, Luo XR, Wen ML et al (2014) Prospecting for concealed copper polymetallic deposit by geo-electrochemical method in forest and marsh covered area—a case study in Tong shan copper deposit, Heilongjiang. J Guilin Univ Technol 34(03):439–445 **(in Chinese with English abstract)**

Zhang YJ, Luo XR, Duan HC et al (2015) Application of geo-electro chemical prospecting method for concealed gold deposit in Liushaogou district of West Qinling Origen. J Guilin Univ Technol 35(03):473–481 **(in Chinese with English abstract)**

Zheng YY, Su X, Tian LM et al (2004) Mineralization, deposit type and metallogenic age of the gold antimony polymetallic belt in the eastern part of north Himalayan. Earth Sci 38(01):108–118 **(in Chinese with English abstract)**